Cleavage Fracture of Large Specimens Containing Small Underclad Cracks

M. BETHMONT, D. MOINEREAU, G. ROUSSELIER
Electricité de France, Moret sur Loing, France

ABSTRACT

Large specimens are tested at low temperature (−170°C) under four point bending until fracture by cleavage occurs. They contain sub-surface underclad cracks or surface cracks. The toughness KIc of the base material is evaluated in the range of 40 and 55 MPa√m. The stress intensity factor KI is computed for each specimen, using several methods. In the calculations, the cracks are alternatively assumed as surface or sub-surface cracks. The values KI computed at maximum applied moment are compared with toughness of the base material. Results show that the calculations in which actual sub-surface cracks are considered as surface cracks lead to too a conservative prediction of fracture. On the other hand, if the assumptions of sub-surface cracks with plastic corrections as proposed by the French procedure are taken, the prediction of fracture is in good agreement with experimental results. Furthermore, it is demonstrated that the effect of the residual stresses due to clad layering is negligible, in the case of sub-surface cracks.

1 INTRODUCTION

Integrity assessment of PWR reactor pressure vessels requires to verify their resistance to fast fracture. With this aim, several fracture mechanics analyses and criteria can be used. The safety of the analyses depends on the "conservatism" of the analysis assumptions. One of these assumptions is the location and the shape of the inital reference defects. In the French procedure (Pellissier Tanon et al. 1990) based on (RCC-M code), the reference defects are assumed to be located just under or within the cladding at the inner side of the vessel; they are not considered as surface cracks but as sub-surface underclad cracks. Their innocuity is deduced from an analysis based on linear elastic fracture mechanics. In addition to classical Irwin plastic zone correction, a specific correction is introduced to take into account the plastic deformation of the cladding. Furthermore, other candidate methods, more sophisticated, have been developped to evaluate more accurately the risk of fracture of pressure vessels in the case of complex loading (i.e. elastic-plastic computations and local approach of fracture).

In order to validate the methods which could be used and evaluate their conservatism, an experimental and numerical study is being carried out by Electricité de France (EDF). Large specimens containing underclad and surface cracks are tested under bending. Test results are interpreted by different methods (Moinereau et al. 1990).

This paper is dealing with the description and the interpretation of some results of this programme. Particularly, it aims at comparing the conservatism of the analyses that would consider the actual sub-surface cracks as surface cracks. Moreover, the validity of the plasticity corrections is studied as well as the effect of residual stresses in the cladding.

SMiRT 11 Transactions Vol. G (August 1991) Tokyo, Japan, © 1991

2 DESCRIPTION OF THE TESTS

2.1 Specimens

Tests on three large specimens under four-point bend loading are described in this paper. Two of these specimens (DSR1 and DSR4) contain small underclad cracks and the third one (DD1) a deeper surface crack. The dimensions of the specimens are given in Fig. 1. The central part of the specimens is cut from a vessel shell ring in A508 Cl3 forged ferritic steel. The two layers cladding – the first one in 309L stainless steel and the second one in 308L – is representative of the cladding of pressure vessels. A stress relief heat is applied on each specimen at 600°C during 8 hours. The cracks are obtained by fatigue at room temperature. The range of the cyclic stress intensity factor imposed at the end of crack growth is equal to 20 MPa√m.

2.2 Test conditions

The tests have been carried out at a temperature of about −170°C. At this temperature, the low toughness of the material is wanted to be representative of the pressure vessel material toughness at the end of life (after embrittlement by irradiation). The load–point displacement is controlled at a rate of 1.5 mm/min until the fracture of the specimen occurs.

The data collected during the tests are: the bending moment (derived from the load), load–point displacement, strains and temperatures. Strains are measured by means of strain gages located on the cladding surface (in tension) and on the opposite surface (in compression). Thermocouples are located on the surface and inside of the specimen to evaluate the temperature evolution during the whole test.

3 MATERIAL CHARACTERIZATION

The tensile properties of the base material (A508 Cl 3) and the ones of the cladding are given in Table I. The base material toughness is determined at different temperature between −196°C and −50°C: the values KIc (or KIJ, derived from JIc) are plotted on Fig. 2. At the test temperatures (about −170°C), KIc is approximately ranging from 40 to 55 MPa√m. The measurement of the ductile tearing resistance of the cladding (J–R curves) has not yet been done. Only Charpy–U results are available at the test temperature. Roughly, from correlations with Charpy–U, KIJ can be assumed to be higher than 100 MPa√m.

4 EXPERIMENTAL RESULTS

For the three specimens, the applied bending moment is plotted in Fig. 3 as a function of the load–point displacement. The curves are linear, showing that fracture occurs in small scale yielding conditions. The strain, measured on the surface of the cladding of DSR4 specimen, is plotted as a function of the applied moment in Fig.4. It can be seen that the maximum strain is about 0,3 %. The behaviour of the cladding is not purely elastic but in first approximation the plasticity is neglected.

At the maximum load the specimens break in two parts, releasing a large amount of energy. The fractographic examinations of the cracked surface show that the fracture of the specimen is entirely due to cleavage without other mode of fracture (Fig. 5). In the case of DD1 specimen it has been observed that crack initiates just near the interface between base material and cladding. On the other specimens, crack initiation can not be pointed out precisely. The instability of the crack occurs immediately after cleavage initiation. So, the maximum applied moment M_{max} (indicated on Fig. 3) corresponds to this crack initiation. The dimensions of the precracked defects (Fig 6) are directly measured on the cracked surfaces.

5 INTERPRETATION OF THE TESTS

5.1 Mechanical analyses

The objective of the analyses described in this paper is to evaluate the stress intensity factor KI by different methods, detailed hereunder, and to compare the results.

- *method A*: assuming unbounded long surface cracks, KI is derived from the formulae proposed by (Tada et al.1973).
- *method B*: assuming semi-elliptical surface cracks, KI is derived, as a function of the position on the crack front, from formulae proposed by (Newman et al. 1981).
- *method C*: two dimensional finite element computation is performed, in linear elastic conditions, to simulate the sub-surface cracks under the cladding. KI is directly deduced from the crack tip opening computation. Irwin plastic zone correction is made to take into account plasticity at the crack tip. Additionnaly, KI is corrected to take the plasticity of the remaining ligament into account: KI is multiplied by a factor α depending of the plastic zone radius r and the ligament b between the crack tip and the clad surface. The lowest boundary value is $\alpha = 1$ if $r < 0.05$ b and the highest value is $\alpha = 1.6$ if $r > 0.085$ b.
- *method C'*: is equivalent to method C but residual stresses in the cladding are taken into account. They are added to the mechanical stresses due to four-point bend loading. Magnitude of residual stresses has been obtained by an elastic-plastic numerical simulation of the cooling process after the stress relief heat treatment. In this calculation, the specimen is assumed to be free of stress at the anneal temperature of 600°C.
- *method D*: two dimensional finite element computation is performed in elastic-plastic conditions. KI is deduced from path-independent J-Integral.
- *method D'*: is equivalent to method D but residual stresses in the cladding are taken into account.

5.2 Test analyses

The stress intensity factor KI is evaluated for each specimen at the level of the maximum applied moment by some of the methods described in § 5.1. The crack dimensions considered in the analyses are detailed in Fig. 6.

- DD1 specimen: the highest value KI = 84 MPa√m is given by method A (see Fig. 7). According to method B, KI is calculated along the initial crack front. The semi-circular surface crack shape is assumed; the maximum value (51 MPa√m) is obtained at the surface and the minimum value (32 MPa√m) at the deepest point. This explains that the crack initiation does not occur at the deepest point but in the base material at the interface with the cladding where KI = 48 MPa√m.

- DSR1 and DSR 4 specimens: the results are presented in table II. The highest value KI is obtained from method A. To calculate KI following method B, the dimensions of the semi-elliptical surface cracks are estimated from an extrapolation of the actual crack measurements. Here, the stress intensity factor is larger at the deepest point. The sub-surface underclad crack analysis is presently limited to two dimensionnal finite element computations. The comparison of the results of elastic analysis (method C) with elastic-plastic analysis (method D) shows a good agreement in the case of DSR4 specimen. On the other hand, in the case of DSR1 specimen with a thinner cladding ligament (5mm), the plasticity correction leads to overestimate KI (with $\alpha = 1.6$). The effect of residual stresses is only investigated on DSR4 specimen: tension stresses in cladding are assumed to be equal to 160 MPa and the base material free of residual stresses. This effect appears to be negligible.

5.3 Discussion: fracture predictions

The results given in § 5.2. can be used to evaluate the conservatism of the different methods that evaluate KI. The values KI are compared to the toughness material KIc. If the crack shape is semi-circular or semi-elliptical, only the maximum value KI_{max}, determined along the whole crack front, is considered. This procedure means the crack initiation occurs if "local" KI is equal to KIc. KIc is choosen as the minimum value determined at the test temperature (40 MPa√m). In table III, the results are given in term of f which is equal to the ratio: KI/KIc. This ratio can be also considered approximately as the ratio of the true maximum applied moment to its value predicted by the analysis. In each case, the unbounded surface crack geometry is a very conservative assumption (f = 2); even for DD1 specimen containing a surface crack. In this latter case, the fracture is very well predicted with the semi-circular crack geometry (f = 1.2).

Unbounded as well as semi-elliptical surface cracks are too conservative assumptions for DSR1 and DSR4 specimens. On the other hand, the two dimensional computations with sub-surface geometry is a better method to predict the specimen fracture with a good accuracy. However, in case of the DSR1 specimen the method based on plastic corrections still seems conservative. This is due to the factor α = 1.6 wich is proposed in French procedure.

As an example, Fig.3 indicates the predicted values of applied moment at fracture of DSR4 specimen, depending of the analysis methods .

Remark : the objective in this paper, is to compare the predictions of specimen fracture load according to the computation methods. This is the reason why KIc is the true toughness, determined on laboratory specimens. In fact, in safety analysis, KIc should be evaluated from the values given in the RCC-M code (which are equivalent in ASME code). This procedure introduces another safety factor on material properties which is not discussed here.

6 CONCLUSION

Electricité de France (EDF) is carrying out an experimental and numerical study in order to validate and evaluate the conservatism of the different methods which can be used in pressure vessels safety analysis. The study includes four-point bending tests on large specimens containing surface or sub-surface underclad cracks. Test results are interpreted using several methods with different crack shape assumptions.

Results show that, if defects are sub-surface underclad cracks, the calculations in which cracks are considered as surface cracks lead to too a conservative prediction of fracture. On the other hand, the analysis, proposed by the French procedure, based on linear elastic mechanics with the assumptions of sub-surface cracks and plastic corrections, leads to a good adequacy with experimental results. Moreover, if plasticity of cladding is not negligible, this analysis becomes much more conservative. Furthermore, it is demonstrated that the effect of the residual stresses due to clad layering is negligible in the case of sub-surface cracks.

REFERENCES

Pellissier Tanon A., Grandemange J., Houssin B. and Buchalet C. (1990) French Verification of PWR Vessel Integrity, Final report EPRI NP-6713.

RCC-M (1988), Design and Construction Rules for Mechanical Components of PWR Nuclear Islands, AFCEN Edition, Paris (available in English).

Moinereau D., Bethmont M., Debruyne G. and Rousselier G. (1990), Brittle Fracture Behaviour of Cracks in Reactor Pressure Vessel. EDF Programme's Presentation. First Testings and Interpretation by Fracture Mechanics, Pressure Vessels and Piping Conference, Nashville.

Tada H., Paris P. and Irwin G. (1973), The Stress Analysis of Cracks Handbook, Hellertown, Pennsylviana, Del Research Corporation.

Newman J.C. and Raju I.S. (1981), An empirical Stress Intensity Factor Equation for the Surface Crack, Engineering Fracture Mechanics, Vol. 15, pp. 185–192.

TABLE I – BASE MATERIAL AND CLADDING TENSILE PROPERTIES AT THE TEMPERATURE OF – 170°C

	Rp0,2 (MPa)	Rm (MPA)	A (%)	Z (%)	E (MPa)
Base material	774	918	26	64	220
Cladding	340	760	15	14	160

TABLE III – EVALUATION OF f FACTOR ($f = K_I / K_{IC}$)

Analysis assump-tions	Surface crack		Sub-surface crack	
	Unbounded crack	Semi-elliptical crack	Elastic analysis + plastic corrections	Elastic-plastic analysis
DD 1	2.2	1.2	–	–
DSR 1	2.3	1.9	1.7	1.3
DSR 4	2.4	2.0	1.1	1.1

TABLE II – STRESS INTENSITY FACTOR EVALUATIONS AT MAXIMUM LOAD FOR DSR 1 AND DSR 4 SPECIMENS (in MPa $\sqrt{m}$)

Analysis assump-tions	Surface crack			Sub-surface crack (two dimensional finite element computation)			
	Unboun-ded crak	Semi-elliptical crack		Elastic analysis + plastic corrections		Elastic-plastic analysis	
				Without r.s.	With r.s.	Without r.s.	With r.s.
Method number	A	B	B'	C	C'	D	D'
DSR 1 specimen	91	76	54	69 (1.60)	–	52	–
DSR 4 specimen	97	79	59	42 (1.03)	46 (1.16)	43	45

r.s. = residual stresses ( ) = α factor

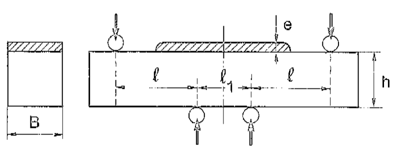

	DD 1	DSR 1	DSR 4
h	127	124	127
ℓ	500	500	600
ℓ_1	450	450	250
B	140	145	150
e	8	5	8

Figure 1 – Four point bending tests : specimen dimensions (in mm).

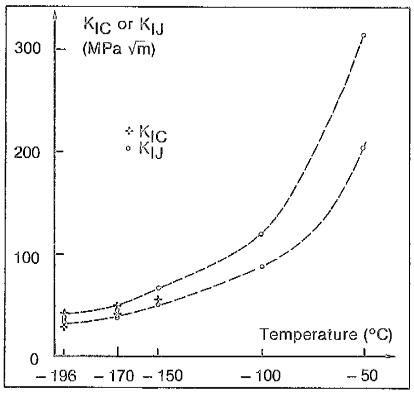

Figure 2 – Base material toughness versus temperature.

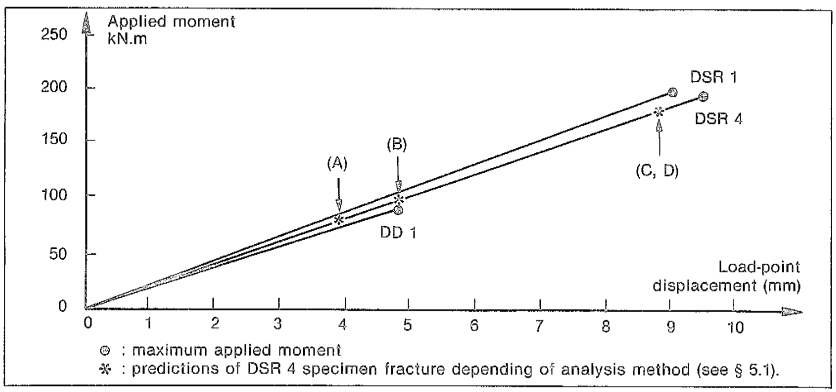

Figure 3 – Applied moment versus load-point displacement.

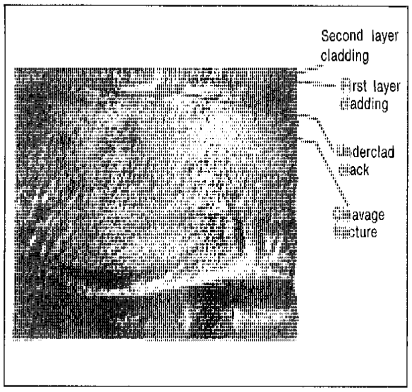

Figure 4 – Fractographic view of DSR 4 cracked surface.

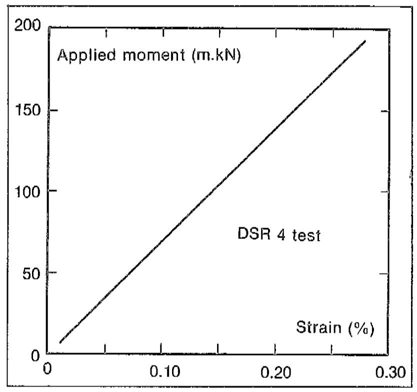

Figure 5 – Applied moment versus cladding strain.

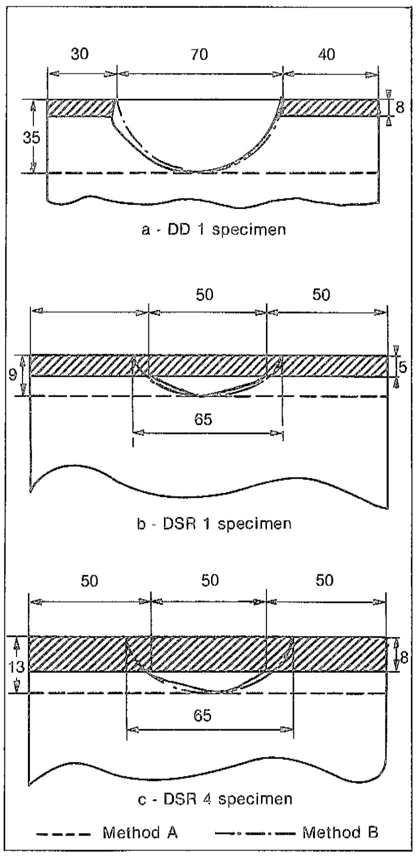

Figure 6 – Crack geometries for K_I computation.

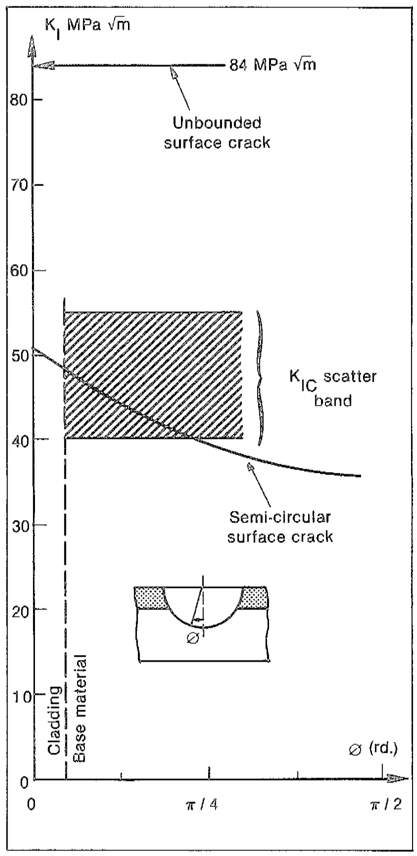

Figure 7 – Stress intensity fractor K_I calculated at maximal load of DD 1 specimen.